J|A|C|S
ARTICLES
Published on Web 10/19/2007

Size Control of Gold Nanocrystals in Citrate Reduction: The Third Role of Citrate

Xiaohui Ji,[†,‡] Xiangning Song,[†] Jun Li,[†] Yubai Bai,[†] Wensheng Yang,*[,†] and Xiaogang Peng*[,‡]

Contribution from the Key Laboratory for Supramolecular Structures and Materials, College of Chemistry, Jilin University, Changchun 130012, P. R. China, and Department of Chemistry & Biochemistry, University of Arkansas, Fayetteville, Arkansas 72701

Received June 18, 2007; E-mail: wsyang@mail.jlu.edu.cn; xpeng@uark.edu

Abstract: Growth kinetics and temporal size/shape evolution of gold nanocrystals by citrate reduction in boiling water were studied systematically and quantitatively. Results reveal that the size variation and overall reaction mechanism were mostly determined by the solution pH that was in turn controlled by the concentration of sodium citrate (Na_3Ct) in the traditional Frens's synthesis. This conclusion was further confirmed by the reactions with variable pH but fixed concentrations of the two reactants, $HAuCl_4$ and Na_3Ct. Two substantially different reaction pathways were identified, with the switching point at pH = 6.2−6.5. The first pathway is for the low pH range and consists of three overlapping steps: nucleation, random attachment to polycrystalline nanowires, and smoothing of the nanowires via intra-particle ripening to dots. The second pathway that occurred above the pH switching point is consistent with the commonly known nucleation-growth route. Using the second pathway, we demonstrated a new synthetic route for the synthesis of nearly monodisperse gold nanocrystals in the size range from 20 to 40 nm by simply varying the solution pH with fixed concentrations of $HAuCl_4$ and Na_3Ct. The switching of the reaction pathways is likely due to the integration nature of water as a reaction medium. In the citrate reduction, the solution pH was varied by changing the initial $HAuCl_4/Na_3Ct$ ratio. Consequently, when pH was higher than about 6.2, the very reactive $[AuCl_3(OH)]^-$ would be converted to less reactive $[AuCl_2(OH)_2]^-$ and $[AuCl(OH)_3]^-$.

Introduction

Growth of monodisperse nanocrystals with controlled sizes is vital for both fundamental science and technical applications. Synthesis of gold nanocrystals in aqueous solution described by Faraday[1] is probably the first well-documented example along this direction. Since then, synthesis of other types of noble metal nanocrystals[2−7] and, lately, growth of size- and shape-controlled gold nanocrystals through seeded growth[8−10] have also been developed in water. However, the quality of these nanocrystals grown in water in terms of size, shape, and size/shape distribution has been significantly lower than that of those high-quality nanocrystals grown in nonaqueous solutions under elevated temperatures, such as the typical II−VI semiconductor nanocrystals.[11,12] Meanwhile, high-quality gold nanocrystals[13−17] have also been synthesized in nonaqueous solvents. From a green chemistry standpoint, however, all of these nonaqueous synthetic schemes are far from ideal. A recent report indicates that the growth temperature of high-quality CdSe nanocrystals can be reduced from 250 to 350 °C to 100−200 °C,[18] which indicates that water may eventually become a plausible medium for the growth of high-quality nanocrystals with various compositions. This attractive future will likely come with systematic and quantitative studies of some carefully chosen aqueous model systems.

Synthesis of gold nanocrystals by citrate reduction is a good model system, which includes only three starting materials, namely, auric acid, sodium citrate, and water. Since it was reported by Turkevich et al. in 1951,[19] this synthetic scheme has been widely studied and a substantial amount of important information regarding this system has been deposited in

[†] Jilin University.
[‡] University of Arkansas.

(1) Faraday, M. *Philos. Trans. R. Soc. London* **1857**, *147*, 145.
(2) Henglein, A.; Giersig, M. *J. Phys. Chem. B* **1999**, *103*, 9533−9539.
(3) Teranishi, T. H. M.; Tanaka, T.; Miyake, M. *J. Phys. Chem. B* **1999**, *103*, 3818−3827.
(4) Henglein, A. *J. Phys. Chem. B* **2000**, *104*, 1206−1211.
(5) Henglein, A.; Giersig, M. *J. Phys. Chem. B* **2000**, *104*, 6767−6772.
(6) Pillai, Z. S.; Kamat, P. V. *J. Phys. Chem. B* **2004**, *108*, 945−951.
(7) Xiong, Y. C. H.; Wiley, B. J.; Wang, J.; Kim, M. J.; Xia, Y. *J. Phys. Chem. B* **2007**, *129*, 3665−3675.
(8) Jana, N. R.; Gearheart, L.; Murphy, C. J. *J. Phys. Chem. B* **2001**, *105*, 4065−4067.
(9) Murphy, C. J.; Jana, N. R. *Adv. Mater. (Weinheim, Ger.)* **2002**, *14*, 80−82.
(10) Nikoobakht, B.; El-Sayed, M. A. *Chem. Mater.* **2003**, *15*, 1957−1962.
(11) Murray, C. B.; Kagan, C. R.; Bawendi, M. G. *Annu. Rev. Mater. Sci.* **2000**, *30*, 545−610.
(12) Peng, X.; Thessing, J. *Struct. Bonding (Berlin)* **2005**, *118*, 79−119.
(13) Lin, X. M.; Sorensen, C. M.; Klabunde, K. J. *J. Nanopart. Res.* **2000**, *2*, 157−164.
(14) Stoeva, S.; Klabunde, K. J.; Sorensen, C. M.; Dragieva, I. *J. Am. Chem. Soc.* **2002**, *124*, 2305−2311.
(15) Jana, N. R.; Peng, X. *J. Am. Chem. Soc.* **2003**, *125*, 14280−14281.
(16) Hiramatsu, H.; Osterloh, F. E. *Chem. Mater.* **2004**, *16*, 2509−2511.
(17) Zheng, N.; Fan, J.; Stucky, G. D. *J. Am. Chem. Soc.* **2006**, *128*, 6550−6551.
(18) Pradhan, N.; Reifsnyder, D.; Xie, R.; Aldana, J.; Peng, X. *J. Am. Chem. Soc.* **2007**, *129*, 9500−9509.
(19) Turkevich, J.; Hillier, J.; Stevenson, P. C. *Discuss. Faraday Soc.* **1951**, *11*, 55.

literature.[19−23] Frens[20] clearly demonstrated that the size variation of the resulting gold nanocrystals by the citrate reduction can be readily realized by simply changing the concentration of sodium citrate. It was suggested that gold nanocrystals were grown through a fast nucleation process followed by a diffusion-controlled growth.[19,20] The size and size distribution of the resulting nanocrystals are thus controlled in a way similar to the well-known Lamar model, which is also known as "focusing of size distribution" in the field of nonaqueous solution synthesis of nanocrystals under elevated temperatures.[24] A very recent work tried to account this mechanism for Frens's synthesis by a theoretical model.[25]

This nucleation-growth mechanism,[19,20,25] however, was found to be contradictory with the temporal evolution of the nanocrystal sizes under certain conditions.[21] Instead of a gradual growth of the nanocrystals, aggregation of nanocrystals was observed at relatively low reaction temperatures (60−80 °C)[21] as well as in boiling water.[22,23] On the basis of their series of experiments at 60−80 °C,[21,26−28] Zukoski and co-workers proposed a reversible aggregation of unstable primary particles in the beginning followed by a redispersion of these primary particles in the final stage of the reaction. Different from the "fluffy", nondense, and spherical aggregates observed in Zukoski's experiments, aggregates found in boiling water were dense solid, crystalline, and wirelike.[27]

Among all of the existing literature on growth of gold and other noble metal nanocrystals by citrate reduction, the dual role of citrate, reducing reagents, and protection groups (or ligands)[2,25−28] has been well identified. However, sodium citrate is a known weak base, which should change the solution pH to a certain extent if its concentration varies. It is known that the reactivity of the gold complexes, reflected by their reduction potential, changes markedly by varying pH.[29] In addition, the molecular forces between citrate protection groups and gold surfaces and ζ-potential of gold nanocrystals were reported to be also strongly dependent on pH.[27,29] Furthermore, Henglein and Giersig[5] did observe some significant effects on synthesis of silver nanocrystals by adding NaOH into the reaction system, clearly indicating the influence of pH on the growth of the nanocrystals. As mentioned earlier, the most popular method developed by Frens[20] for controlling the size of the noble metal nanocrystals by citrate reduction is based on varying the concentration of sodium citrate. These thoughts invited us to systematically examine the role of sodium citrate as a pH mediator in the growth of gold nanocrystal, which is the main theme of this work. To better address this issue and clarify differences from the other two roles of citrate, a significant portion of the experiments and result analysis was carried out in a quantitative manner.

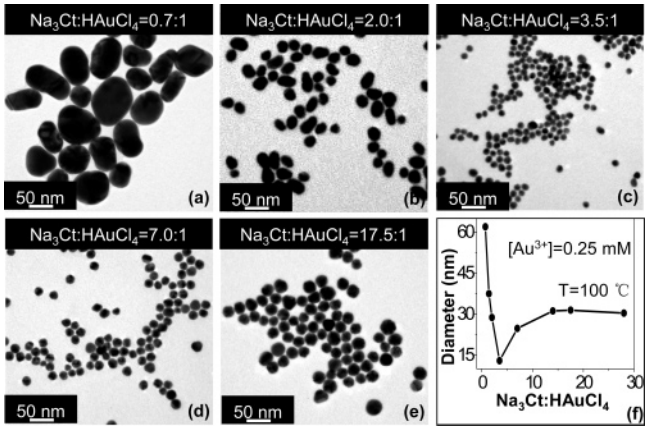

Figure 1. TEM images (a−e) and summary (f) of the average sizes of gold nanocrystals synthesized using different $Na_3Ct/HAuCl_4$ precursor ratios as labeled in each image. All nanocrystals were grown in boiling water using an initial $HAuCl_4$ concentration of 0.25 mM.

Results

The size variation of gold nanocrystals through standard citrate reduction in boiling water[20] (Figure 1, top row) was reproduced by varying the initial molar ratio between sodium citrate (Na_3Ct) and auric acid ($HAuCl_4$), the $Na_3Ct/HAuCl_4$ ratio. The $HAuCl_4$ concentration was examined between 0.125 and 1 mM, and the general trend was found to be similar. Unless pointed out specifically, the auric acid concentration was set as 0.25 mM for the results to be discussed here. Because of the fixed auric acid, the $Na_3Ct/HAuCl_4$ ratio also reflects the concentration of Na_3Ct for a specific reaction.

In the original nucleation-growth mechanism proposed, the nucleation rate of Au nanocrystals was thought to increase when the concentration of Na_3Ct increased either as the reducing reagent[19,20] or as the precursor of a stabilization reagent for Au^+ ions.[25] In any case, the number of nuclei should increase as the concentration of the sodium citrate increased. After this initial fast nucleation, the number of nanocrystals should keep constant in the following diffusion-controlled growth. Therefore, the final size of the nanocrystals after all monomers were consumed should decrease as the concentration of sodium citrate increased, provided that the precursor concentration was fixed. This seems to be consistent with the results shown in the first row of Figure 1.

However, further increase of the $Na_3Ct/HAuCl_4$ ratio, from 3.5:1 in traditional Frens's method[20] to 28:1, violated the increasing trend of the average sizes predicted by the nucleation-growth mechanism. Instead of a continuous reduction of the particle size, the size of the final products actually showed a significant increase and leveled off (see transmission electron microscope (TEM) images in the second row in Figure 1). Figure 1f summarized the overall trend of the size variation upon changing the $Na_3Ct/HAuCl_4$ ratio under the given $HAuCl_4$ concentration. It should be pointed out that a similar nonmonotonic size variation was also observed for the growth of Ag nanocrystals through a γ-radiation-induced reduction using Na_3Ct as the protection reagent.[2]

Although the trend of size variation of the final gold nanocrystals in the low $Na_3Ct/HAuCl_4$ ratios was found to be

(20) Frens, G. *Nature (London), Phys. Sci.* **1973**, *241*, 20−22.
(21) Chow, M. K.; Zukoski, C. F. *J. Colloid Interface Sci.* **1994**, *165*, 97−109.
(22) Kimling, J.; Maier, M.; Okenve, B.; Kotaidis, V.; Ballot, H.; Plech, A. *J. Phys. Chem. B* **2006**, *110*, 15700−15707.
(23) Pong, B.-K.; Elim, H. I.; Chong, J.-X.; Ji, W.; Trout, B. L.; Lee, J.-Y. *J. Phys. Chem. C* **2007**, *111*, 6281−6287.
(24) Peng, X.; Wickham, J.; Alivisatos, A. P. *J. Am. Chem. Soc.* **1998**, *120*, 5343−5344.
(25) Kumar, S.; Gandhi, K. S.; Kumar, R. *Ind. Eng. Chem. Res.* **2007**, *46*, 3128−3136.
(26) Biggs, S.; Chow, M. K.; Zukoski, C. F.; Grieser, F. *J. Colloid Interface Sci.* **1993**, *160*, 511−513.
(27) Biggs, S.; Mulvaney, P.; Zukoski, C. F.; Grieser, F. *J. Am. Chem. Soc.* **1994**, *116*, 9150−9157.
(28) Wall, J. F.; Grieser, F.; Zukoski, C. F. *J. Chem. Soc., Faraday Trans.* **1997**, *93*, 4017−4020.
(29) Goia, D. V.; Matijevic, E. *Colloids Surf., A* **1999**, *146*, 139−152.

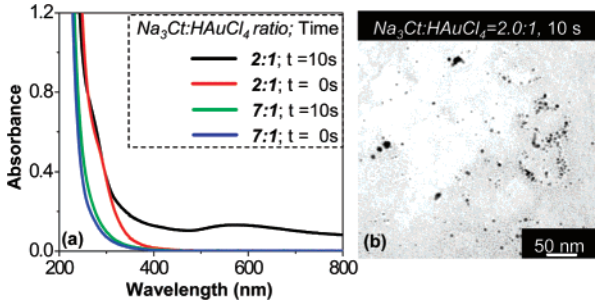

Figure 2. Left: UV−vis spectra of the reaction mixtures for two different precursor ratios before and 10 s after the reaction. Right: TEM image for the 10-s sample when the precursor ratio was 2:1.

consistent with the original nucleation-growth model, some careful examinations to be described here indicate that this model contradicts with experiments on several aspects even in this small $Na_3Ct/HAuCl_4$ ratio range used by Frens.[20] Figure 2 (left) illustrates the UV−vis absorption spectra of the reaction mixtures for two different $Na_3Ct/HAuCl_4$ ratios before (0 s) and immediately after (10 s) the reaction was initiated. To avoid reaction, the spectra at 0 s were recorded by mixing all reactants at room temperature without heating. The spectra clearly indicate that a rapid change upon the addition of Na_3Ct was observed for the reaction with a low $Na_3Ct/HAuCl_4$ ratio. Specifically, a noticeable absorption feature at around 550 nm appeared in the spectrum at 10 s, indicating the formation of Au particles. Conversely, there was barely any change detectable in the same time frame for the reaction with a high $Na_3Ct/HAuCl_4$ ratio. This means that the nucleation rate actually decreased as the $Na_3Ct/HAuCl_4$ ratio increased, which is opposite to what was expected for the nucleation-growth model. Furthermore, this indicates that the role as a reducing reagent of citrate is unlikely controlling the nucleation process.

Consistent with this spectroscopic evidence, a significant amount of relatively small gold nanocrystals with a quite broad size distribution was observed under TEM immediately (10 s) after the injection of Na_3Ct for the reaction with $Na_3Ct/HAuCl_4$ ratio being 2:1 (Figure 2, right). Conversely, there were no particles observed at the same reaction time for the reaction with $Na_3Ct/HAuCl_4$ ratio at 7:1. In fact, it took about 60 s for the reaction to produce some small particles detectable by TEM (Figure 3a).

The temporal evolution of the size and shape of gold nanocrystals was examined for several reactions with selected $Na_3Ct/HAuCl_4$ ratios using TEM. In general, there are two distinguishable evolution patterns (Figure 3).

For a reaction with a relatively high $Na_3Ct/HAuCl_4$ ratio (higher than 3.5:1), the general evolution trend is similar to that represented by the 7:1 ratio (Figure 3, top row). In this Na_3Ct concentration (or $Na_3Ct/HAuCl_4$ ratio) range, the initiation rate of the reaction, judged by the appearance of observable gold nanocrystals under TEM and spectroscopic deviation from the original precursor solutions, was generally slow (Figure 2 and the related text). After the initial nucleation, the average size of the nanocrystals increased with time until it reached a stable size, which took about 10 min. In most cases, single and close to spherical particles were the major products, although some small aggregates, such as dimers and trimmers, might be observed (Figure 3b). As the $Na_3Ct/HAuCl_4$ ratio increased, the tendency of aggregation decreased. Overall, the growth pattern in this $Na_3Ct/HAuCl_4$ ratio range seems to be consistent with a nucleation-growth model, which will become more apparent after we examine the temporal evolution of optical spectra and monomer concentration quantitatively later in this article. However, it should be pointed out that the size variation in this $Na_3Ct/HAuCl_4$ ratio window did not follow the original nucleation-growth model.[19] As shown in Figure 1f, instead of a decrease in their average size upon increasing the $Na_3Ct/HAuCl_4$ ratio, an opposite trend was observed.

For the reactions in the low $Na_3Ct/HAuCl_4$ ratio window (below 3.5:1), which covers almost the entire range of the traditional Frens's approach for size variation,[20] the representative pattern of the temporal size/shape evolution of the gold nanocrystals is shown in Figure 3 (bottom row). Different from the high ratio reactions, appearance of small gold nanocrystals was instantaneous within the experimental resolution (Figure 2 and the related text). Subsequently, these small gold nanocrystals evidently started to form aggregates, most of the aggregates being in irregular wire shape. These wirelike aggregates were crystalline and dense solid (see high-resolution TEM (HRTEM) results later) and are similar to that observed in a few recent reports[22,23,30] but different from the fluffy and spherical aggregates yielded under a relatively low reaction temperature.[21] The length and degree of complexity of those solid wires were found to increase as the $Na_3Ct/HAuCl_4$ ratio decreased. At a very low $Na_3Ct/HAuCl_4$ ratio (0.7:1), the wires were very complex and it was sometimes difficult to distinguish one aggregate from another (Supporting Information, Figure 1S), which is similar to the two-dimensional nanowire network reported by Pei et al.[30] Although these complex aggregates for the reactions with extremely low $Na_3Ct/HAuCl_4$ ratios ($\leq$0.7:1) are both scientifically and technically interesting,[30] the complicity prevented us from choosing them as our targets in this initial work. Instead, we concentrated on the reactions with a medium $Na_3Ct/HAuCl_4$ ratio to illustrate the size/shape evolution of the nanowire aggregates (Figure 3, bottom row).

In Figure 3 (bottom row), one striking structural feature in the intermediate stage is that the diameter of each wire was not uniform, often with a "fat" but solid head (Figure 3f,g). The majority part of a wire was substantially smaller than the fat head (Figure 3f,g) that was further smaller than the size of the final product (Figure 3h).

Consistent with the shape evolution observed by TEM, the temporal evolution of UV−vis absorption spectra of the reaction solutions also possessed two different patterns (Figure 4). For the reactions with a low $Na_3Ct/HAuCl_4$ ratio (Figure 4a,b), rapid appearance of a significant absorbance in the wavelength range in the 600−800-nm window in the early reaction times is consistent with the substantial elongation[31] shown in Figure 3 (bottom row). As expected, the absorption spectrum of the final products slowly lost its absorbance in the 600−800-nm window and ended up with a pronounced absorption peak in the 520−540-nm range, indicating the nearly spherical shape of the final products.[32]

Conversely, the UV−vis absorption spectra at all stages of the gold nanocrystals grown in the reactions with a high Na_3-

(30) Pei, L.; Mori, K.; Adachi, M. *Langmuir* **2004**, *20*, 7837−7843.
(31) Yu, Y.-Y.; Chang, S.-S.; Lee, C.-L.; Wang, C. R. C. *J. Phys. Chem. B* **1997**, *101*, 6661−6664.
(32) Kreibig, U.; Vollmer, M. *Optical Properties of Metal Clusters;* Springer Series in Materials Science 25; Springer: Berlin, 1995.

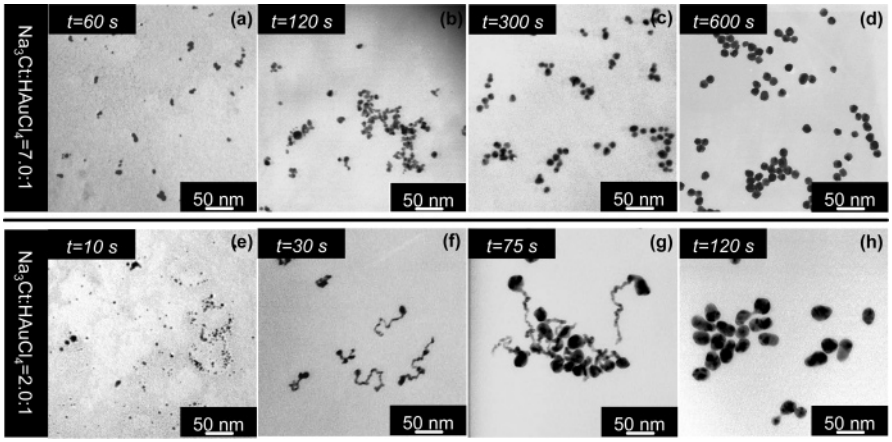

Figure 3. Temporal size/shape evolution of gold nanocrystals using two different precursor ratios as labeled. Note: the time scale is different for the two cases.

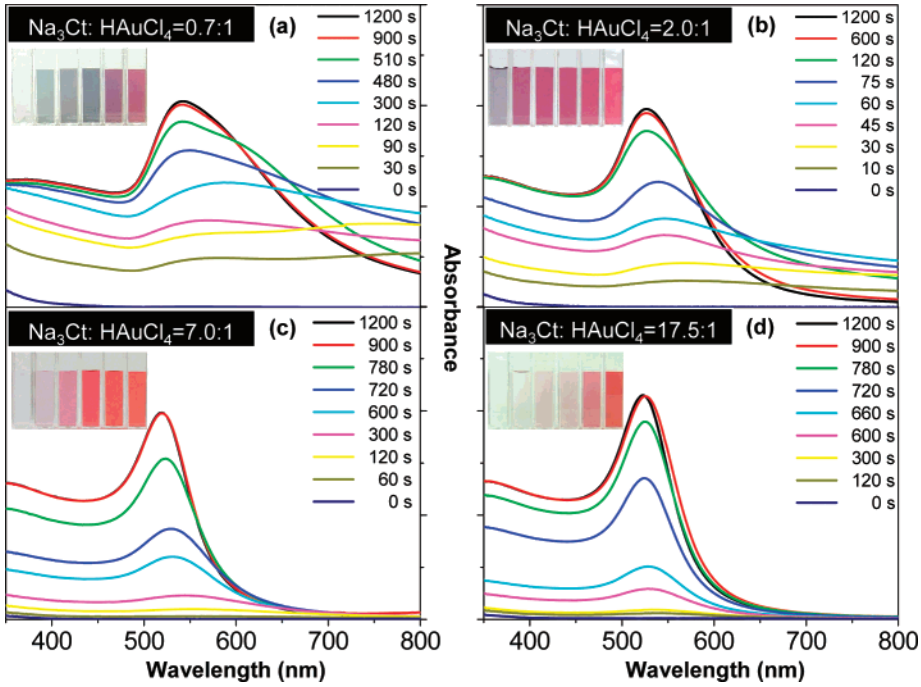

Figure 4. Temporal evolution of UV−vis spectra of four reactions with different precursor ratios as labeled. Inset: photographs of the color evolution for each reaction.

$Ct/HAuCl_4$ ratio (Figure 4c,d) were with characteristic absorption spectra of dot-shaped nanocrystals, a well-defined absorption peak in the 520−540-nm range.[32] This was particularly true in Figure 4d. Again, these results are consistent with the observations by TEM (Figure 3, top row and the related text) in this $Na_3Ct/HAuCl_4$ ratio range that particles maintained mostly as individual dots and tendency of aggregation decreased by increasing the $Na_3Ct/HAuCl_4$ ratio.

The spectroscopic differences between the reactions with a low (Figure 4a,b) and a high (Figure 4c,d) $Na_3Ct/HAuCl_4$ ratio can also be visualized directly. As shown in the inset in each plot in Figure 4, the reactions with a low precursor ratio (Figure 4a,b) showed a quick appearance of blue color in the solution, which is similar to what was originally observed by Frens.[20] Conversely, the reactions with a high precursor ratio (Figure 4c,d) were colorless in the beginning and the wine red was developed gradually.

Although only four sets of temporally resolved UV−vis spectra are shown in Figure 4, reactions with a variety of $Na_3Ct/HAuCl_4$ ratios were studied using this technique. The integrated absorbance in the 600−800-nm window as well as the absorbance at the absorption peak are summarized in Figure 2S for a large collection of reactions. All data in this broad $Na_3Ct/HAuCl_4$ ratio range, from 0.7:1 to 28:1, supported a general conclusion: gold nanocrystals in the reactions with a high $Na_3Ct/HAuCl_4$ ratio grew through a nucleation-growth pathway more or less without particle aggregation, and serious aggregation of primary particles to nanowire-shaped objects occurred for the reactions with a low $Na_3Ct/HAuCl_4$ ratio in the initial stage. The latter case covers the most part of the $Na_3Ct/HAuCl_4$ ratio range for size control in traditional Frens synthesis, which is probably why Frens observed the quick appearance of blue color (elongated aggregates) followed by a color change to wine red.[20]

In the low precursor ratio range, although the nucleation process was almost instantaneous (Figure 2), the absorption spectra actually detected changes for a long period of time (compare the last two spectra in Figure 4a,c). This indicates

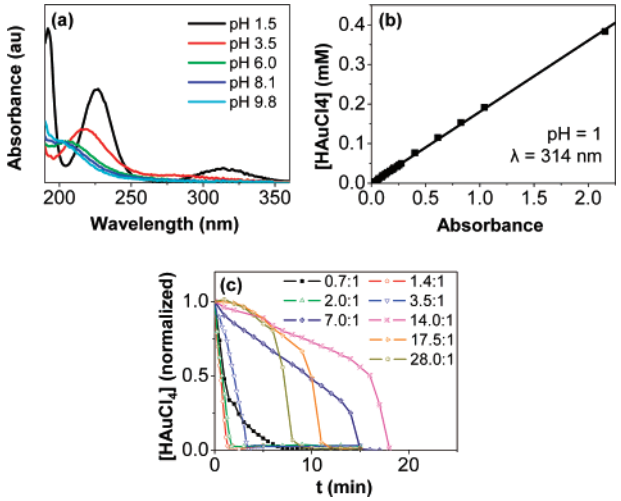

Figure 5. (a) UV absorption spectra of Au(III) complex ions at different pH values. (b) Linear relationship between the absorbance at 314 nm of Au(III) complex ion and its molar concentration at pH = 1. (c) Temporal evolution of Au(III) ion concentration for the reaction with different $Na_3Ct/HAuCl_4$ precursor ratios as labeled.

that the transition of the wire-shaped aggregates to the final nearly spherical dots took an extended period of time. In fact, the resulting nanocrystals using Frens method are often oval-shaped,[20] especially for the ones with a relatively large average size (Figures 1 and 1S).

Temporal evolution of the monomer concentration during the growth of nanocrystals is always a critical piece of information for clarifying the growth mechanism of nanocrystals. Fortunately, the optical spectra of gold(III) complexes have been well studied.[33] It is well known that the structure of the gold complexes changes by varying the solution pH, and these structural changes can be identified by UV−vis spectra (Figure 5, left). Therefore, one simple way to determine the monomer structure and concentration in the solution was to directly compare the absorbance of the corresponding absorption bands. A more quantitative and reliable method would be as follows.

As shown in Figure 5 (left), a sharp absorption peak at 314 nm due to a ligand−metal transition of $[AuCl_4]^-$ complex can be well resolved when the solution pH was below 1.5.[33] The intensity of this peak, measured for different gold ion concentrations, was found to follow Beer's law in a quite broad range of the ion concentration (Figure 5b). This allowed us to determine the gold ion concentration in an aliquot taken at a given time interval for a specific reaction. To do so, the aliquot was immediately quenched by adding it into a preprepared solution of NaCl (0.9 M) and HCl (pH = 1) to obtain a colorless solution at room temperature. The gold ion concentrations determined in this way for a series of reactions with different $Na_3Ct/HAuCl_4$ ratios are shown in Figure 5c.

Although the reaction rates shown by the temporal monomer concentration evolution in Figure 5c differed substantially from one reaction to another, the general trend shows a relatively slow consumption of the gold ions followed by a sudden drop. The only exception was the reaction with the very low $Na_3Ct/HAuCl_4$ ratio, 0.7:1, which had a gradually slowed reaction rate toward the end of the reaction, which should be a result of the too-low concentration of Na_3Ct as the reductant.

(33) Peck, J. A.; Tait, C. D.; Swanson, B. I.; Brown, G. E., Jr. *Geochim. Cosmochim. Acta* **1991**, *55*, 671−676.

The initial reaction rates, indicated by the gold ion consumption in early stages of the reactions in Figure 5c, were substantially faster when the $Na_3Ct/HAuCl_4$ ratio was relatively low in comparison to that for the reactions with high $Na_3Ct/HAuCl_4$ ratios. This nicely matches the general conclusion regarding the nucleation rate difference for the reactions with different $Na_3Ct/HAuCl_4$ ratios shown in Figures 2−4. It further indicates that, by and large, the reaction rates did not increase by increasing the $Na_3Ct/HAuCl_4$ ratio under a fixed gold ion concentration.

The temporal evolution curve of the monomer concentration in Figure 5c was approximately a mirror image of the corresponding temporal evolution of the absorption peak intensity in the UV−vis absorption spectra (Figure 2S). It is known that the extinction coefficient of gold nanocrystals at their absorption peak is proportional to the particle volume.[32] Therefore, one can qualitatively conclude that the gold ions reduced were not accumulated in the solution but were consumed for the nucleation and growth of the nanocrystals. In addition, this fact also implies that the method for determining monomer concentration is quite reasonable.

The tentative mechanism drawn for the reactions with a high $Na_3Ct/HAuCl_4$ ratio, nucleation-growth mechanism, seems to be consistent with the corresponding temporal evolution curves of the monomer concentration (Figure 5c). For example, in Figure 3 (top panel), the size of the nanocrystals increased continuously from 1 min to about 10 min for the reaction with its $Na_3Ct/HAuCl_4$ ratio being 7:1. In the same time period, the monomer concentration was substantial and decreased continuously (Figure 5c).

Conversely, the monomer concentration for the reaction with a low $Na_3Ct/HAuCl_4$ ratio was consumed at an extremely fast pace. For the reaction related to Figure 3 (bottom row), about 80% of Au(III) ions were consumed within the first 75 s, and the monomer concentration for this specific reaction became almost zero about 2 min after the reaction started (Figure 5, right). These two facts have two important implications.

First, it is very unlikely that the final particles for the reactions with a low $Na_3Ct/HAuCl_4$ ratio were originated from the breakdown of the existing wirelike aggregates (Figure 3f,g). The monomers left over would simply be insufficient for the fragments with small diameters (assuming they were similar to that of the wirelike aggregates in Figure 3f,g) to fully develop to the very large final particles in Figure 3h. This holds true no matter whether the spherical particles were cleaved after their full growth or they developed to the final size in solution after the cleavage.[23] It should be mentioned that the amount of monomers needed for a particle to grow is proportional to a cubic function of the size. For example, to double its size of an existing crystal, the monomers needed would be eight times more than the monomers for the formation of the original particle.

Second, for the reaction with the $Na_3Ct/HAuCl_4$ ratio being 2:1, there were no monomers for the growth of nanocrystals roughly 2 min after the reaction initiated (Figure 5, right) as mentioned earlier, but the shape and size of the nanocrystals were evolved for a much longer time as observed by UV−vis (Figures 4b and 2S). This means that the final size and shape evolution was related to the gold atom exchange either between nanocrystals (Oswald ripening) or within a nanocrystal (intra-

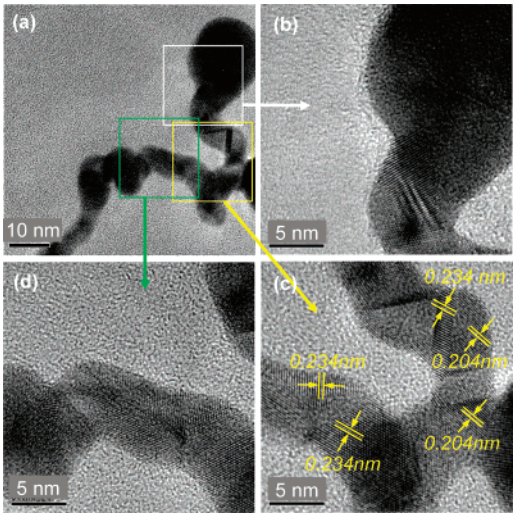

Figure 6. HRTEM images of several sections of a nanowire.

particle ripening).[34] As shown in Figure 2S, this process seems to be intra-particle ripening. This late-stage spectrum evolution is mostly visible by examining the integrated absorbance in the 600−800-nm window, which showed a continuous decrease for this specific reaction (Figure 2S, left) even beyond 10 min of reaction. This means that the nanowire intermediates gradually became dot-shaped at a much slower pace in comparison to the completion of reduction of Au(III) ions. From Figure 3 (bottom row), this intraparticle ripening process basically shortened the skinny tail and made the head fatter and fatter (compare Figure 3f−h). The last statement can also be drawn for the reaction with the $Na_3Ct/HAuCl_4$ ratio being 0.7:1, which has several more TEM images (Figure 1S). For this reaction, the monomers were consumed at about 6−8 min after the reaction proceeded (Figure 5c). However, the TEM measurements (Figure 1S) indicate that the shape of the nanocrystals continued to become more round for at least 15 min.

The dense solid, crystalline, and attachment nature of the wirelike aggregates can be illustrated using HRTEM (Figure 6). A representative nanowire formed in a reaction with its $Na_3Ct/HAuCl_4$ ratio being 2:1, the same as that for the reaction related to the bottom panel in Figure 3, is shown in Figure 6.

Figure 6 illustrates that, along the wire, the nanostructure was dense solid and polycrystalline, with a few locations lacking lattice fringes. Several types of lattice planes with different plane distances are shown in Figure 6c, which indicates the random orientation nature of the nanowires. These results confirmed that the wirelike aggregates observed here were substantially different from the "fluffy", nondense, and spherical aggregates observed by Chow and Zukoski in their reactions carried out under relatively low reaction temperatures.[21] Instead, they were very similar to the nanowires and two-dimensional nanowire networks reported recently.[30]

The domain size of a few distinguishable single crystalline domains can be identified to be in the order of a few nanometers, which was in the same order for the spherical gold nanocrystals observed in the initial stage of the reaction (Figure 3e). These results suggest that such nanowires were formed by random aggregation but not oriented attachment.[35]

(34) Peng, Z. A.; Peng, X. *J. Am. Chem. Soc.* **2001**, *123*, 1389−1395.
(35) Penn, R. L.; Banfield, J. F. *Science (Washington, D. C.)* **1998**, *281*, 969−971.

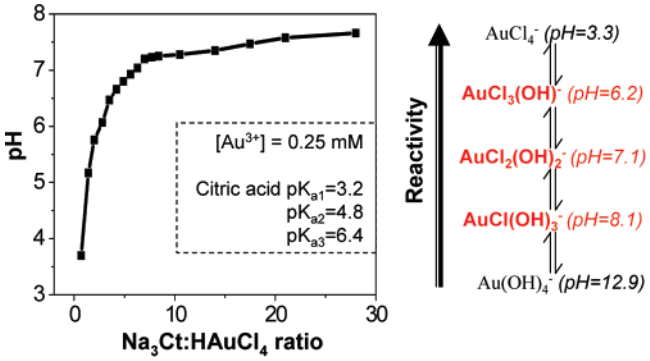

Figure 7. Left: pH variation upon the addition of Na_3Ct in the precursor ratio range used in Figure 1. Right: Structure and reactivity variations of Au(III) complexes upon changing the solution pH. Three dominating species associated with this work are shown in red.

The strong pH-dependent reduction potential of Au(III) complexes, with chloride and/or hydroxide as the ligands, has been well documented in the literature.[29−33] As a key reactant for the formation of gold nanocrystals, its decreased reactivity upon increasing pH might be able to explain the puzzling results on the decreased nucleation rates upon increasing the concentration of Na_3Ct (Figures 2−5).

The above hypothesis, that the pH-dependent reactivity of the Au(III) complex may play a determining role in the current system, is based on the weak base nature of Na_3Ct, which hydrolyzes as a salt from a strong base and weak acid. The three pK_a values of citric acid are known to be 3.2, 4.8, and 6.4, respectively. Therefore, when Na_3Ct was added to the auric acid aqueous solution, it should change the pH of the solution. The final pH of the mixture should depend on the relative concentration of Na_3Ct and auric acid or the $Na_3Ct/HAuCl_4$ ratio. To illustrate this point, the pH values of the reaction solutions were measured at room temperature with the designated solution compositions, that is, a series of $Na_3Ct/HAuCl_4$ ratios (Figure 7, left). Again, the concentration of auric acid was fixed as 0.25 mM. Figure 7 (left) clearly indicates a significant pH change upon adding a different amount of Na_3Ct into the solution with 0.25 mM of auric acid. Noticeably, two reactivity switching points, at pH = 6.2 and 7.1, for Au(III) complexes due to their structural changes are actually in this pH range (Figure 7, right).[29]

In addition to the possible influence on the reactivity of Au(III) complexes, the substantial pH variation in Figure 7 (left) upon changing the $Na_3Ct/HAuCl_4$ ratio may also affect the reactivity of Na_3Ct itself. This is so because the dominating existing form of citrate group shall change upon the strong variation of pH. For example, when pH was above the third pK_a of citric acid, 6.4, the dominating form should be Ct^{3-}. In the pH range associated with the current system, there could be another switching point for the structure of citrate group, which is around pH = 4.8 (the second pK_a of citric acid). Na_3Ct as the reducing reagent was always in large excess (considering its complete oxidation), and also the earlier results (Figures 2−5) revealed that the role as a reducing reagent was not the controlling factor for the formation of the nanocrystals. Therefore, the pH effects in terms of reaction rate might be mostly from Au(III) complexes. However, the pH effects on citrate group as a ligand should still be kept in mind.

With the data in Figure 7 and the earlier analysis, one would conclude that the pH in a reaction solution may have played a

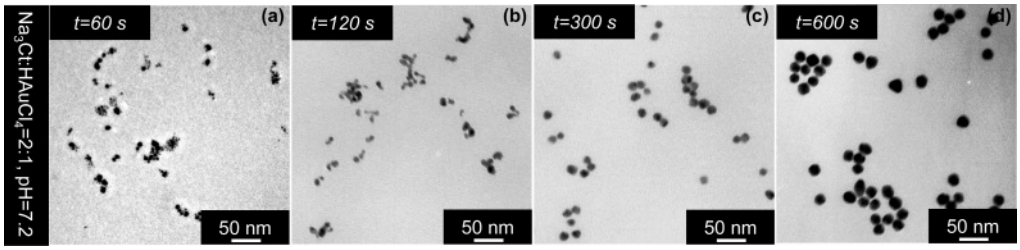

Figure 8. Temporal evolution of the size/shape of gold nanocrystals formed in a reaction with the same precursor ratio (2:1) as the reaction in Figure 3 (bottom row). The pH in this reaction was adjusted to pH = 7.2.

decisive role in determining the reaction rates, the size/shape evolution pattern of the nanocrystals, the final size of the nanocrystals, and so forth. To confirm this hypothesis, further experiments were designed and carried out. As will be shown in the following two subsections, results from these experiments nicely support this hypothesis.

The pH influence on the size/shape evolution of gold nanocrystals was studied for reactions with different pH values but a fixed $Na_3Ct/HAuCl_4$ ratio and initial Au(III) ion concentration (0.25 mM). Figure 8 illustrates the shape/size evolution of one reaction with its pH adjusted. This reaction had the same $Na_3Ct/HAuCl_4$ ratio (2:1) as that for the reaction shown in Figure 3 (bottom row) but the same pH as that of the reaction related to the top row in Figure 3, pH = 7.2. It is interesting to compare these three reactions: two in Figure 3 and one in Figure 8. Please note the time scale difference labeled on each TEM image for a given reaction. It should not be difficult to conclude that the reaction rate and size/shape evolution pattern were both similar for two reactions with the same pH (Figures 3, top row, and 8). In comparison to the reaction with a low pH (Figure 3, bottom row), both reactions with a high pH (Figures 3, top panel, and 8) were quite slow and wirelike aggregations were not dominating in any stage of the reaction (see the earlier text related to Figure 3). Reactions with different $Na_3Ct/HAuCl_4$ ratios showed similar results (see one example in Figure 3S, top row).

The above specific example strongly suggests that the concentration change of Na_3Ct has more influence for the formation of gold nanocrystals as pH mediator than as the reducing reagent. Similarly, the role of Na_3Ct as a ligand also seemed to be less important in comparison to the role as a pH mediator.

To systematically illustrate the pH effects, reactions with a fixed $Na_3Ct/HAuCl_4$ ratio and auric acid concentration but varied pH were studied in the range from pH = 3.7 to pH = 8. It should be pointed out that this pH range was similar to the one encountered by varying the Na_3Ct concentrations shown in Figure 7. When the pH was further lowered, the reaction was too fast to be controlled. Sometimes, the solution would become colorless and some golden-colored flakes were found on the surface of the reaction solution. The reaction would become too slow to study when the pH was adjusted to above 8. The temporal evolution of Au(III) ion concentrations for the reactions with their $Na_3Ct/HAuCl_4$ ratio being 7:1 and auric acid concentration as 0.25 mM is shown in Figure 9a. These results quantitatively and systematically reveal the strong pH dependence of the reaction rates for this synthetic system. If one compares a curve in Figure 9a with the corresponding one in Figure 5c with the same pH, the close similarity of the reaction rates in the early stage could be qualitatively identified.

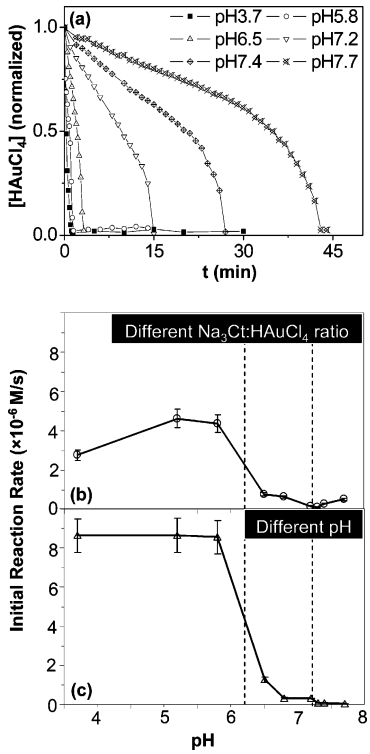

Figure 9. (a) Temporal evolution of Au(III) concentration of the reactions with variable pH at fixed initial Au(III) and Na_3Ct concentrations. (b) Initial reaction rates of Au(III) ion reduction determined for the reactions with variable $Na_3Ct/HAuCl_4$ ratios. (c) Initial reaction rates of Au(III) ion reduction determined for the reactions with a variable pH but a fixed $Na_3Ct/HAuCl_4$ ratio.

Quantitative analysis of the initial reaction rate for each reaction will be given in this article.

The initial reaction rate can be calculated from the temporal evolution of Au(III) ion concentration shown in Figures 5c and 9a. The calculation method relied on fitting the temporal evolution curve of Au(III) ion concentration, with at least eight concentration points for each reaction, into a Taylor expansion (polynomial) with a high confidence (average *R*-squared value for all reactions in Figure 9b,c being 99.3%). The first derivative at time = 0 should thus give the initial reaction rate for each reaction. The obtained values are shown in Figure 9b,c.

The initial reaction rates for the reactions with the same $Na_3Ct/HAuCl_4$ ratio (7:1) but different pH values are shown in Figure 9c. These results show a sharp decrease in the reaction rate at pH = 6.2 and a small drop at around pH = 7.2; both are indicated by two dashed lines. These two transition points were very close to two reactivity switching points of Au(III) complexes in this pH range (Figure 7, right). Conversely, these two transition points were quite far away from the two pK_a

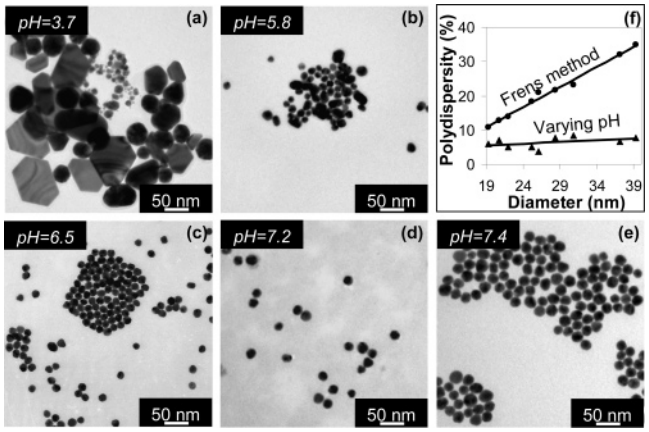

Figure 10. TEM images (a−e) of gold nanocrystals synthesized by varying the pH but with fixed initial Au(III) and Na_3Ct concentrations. (f) Size distribution comparison between the Frens method and the strategy by varying pH with pH ≥6.5 (see detail in text).

values of citric acid in this pH range, 4.8 and 6.4 (Figure 7, left). Specifically, the reaction rates between pH = 4 and 5.8 were found to be almost constant (Figure 9c). It should also be mentioned that the transition point for the size variation by varying either the pH or the $Na_3Ct/HAuCl_4$ ratio (Figure 1f) was found to be around pH = 6.5 (the data were replotted using pH as the *x*-axis in Figure 4S), which seems to be slightly higher in pH than that for the major reaction rate switching point in Figure 7. Interestingly, pH = 6.4 is actually one of the pK_a values of citric acid in this pH range.

The initial rates for the reactions in the series of variable $Na_3Ct/HAuCl_4$ ratios in Figure 9b have a similar pattern but less regular than that in Figure 9c. The differences of the absolute reaction rates between these two sets of data could not be ignored. At low pH values (pH = 3.7 to 5.8 in Figure 9b,c), the reaction rates for a reaction in the variable pH value series (Figure 9c) were substantially higher than that for the corresponding reaction in the variable $Na_3Ct/HAuCl_4$ ratio series (Figure 9b). An opposite trend was observed for the reactions in the pH range higher than pH = 7.2. This is reasonable because two corresponding reactions had the same initial pH and the same initial Au(III) ion concentration, but their reducing reagent (Na_3Ct) concentration in two corresponding reactions could be significantly different. Therefore, an increased reaction rate would be expected for the one with a high Na_3Ct concentration. Consistent with this hypothesis, the equal concentration point was at pH = 7.2. For the same reason, the slight increase in reaction rates in two pH windows, from pH = 3.7 to pH = 5.8 and pH > 7.2, in the variable $Na_3Ct/HAuCl_4$ ratio series (Figure 9b) is also reasonable as the Na_3Ct concentration increased continuously for 40 times as the pH increased in this series. Overall, the reaction rates in Figure 9b for the reactions in the variable $Na_3Ct/HAuCl_4$ ratio series can be considered as the superposition of the variation pattern in Figure 9c and an increasing trend due to the substantial increase of the reducing reagent, with the pH effect pattern as the main course.

Size variation by changing the reaction pH only was also studied. Similar to the trend shown in Figure 1, the final size of the nanocrystals decreased in the beginning as the pH increased, and followed by an increase of the particle size (Figure 10). As the initial Au(III) ion concentration and the $Na_3Ct/HAuCl_4$ ratio were both fixed for the reactions related to Figure 10, one can conclude that the size of gold nanocrystals is strongly related to the reaction pH of the reaction solution. This directly supports the hypothesis that the size variation observed in the original work by Frens[20] should be related to the pH change caused by Na_3Ct as the pH mediator.

Goia and Matijevic reported the crystalline sizes in their largely sized colloidal aggregates in a broad pH range using iso-ascorbic acid as the reducing reagent at room temperature.[29] Their results indicate that a general decreasing trend by increasing pH was observed. It should be noted that the sizes reported in their work were based on XRD measurements of the primary particles inside largely sized aggregates. One may argue that the growth environment and growth pathway for their nanocrystallites were probably quite different from what we studied here.

It is interesting to note that the size distribution of the resulting gold nanocrystals obtained by tuning the reaction pH (Figure 10, bottom row) was significantly better than that obtained by the traditional synthetic scheme by varying the $Na_3Ct/HAuCl_4$ ratio (Figure 1, top row). It should be pointed out that this statement is true only in the size range roughly from 20 to 40 nm and with the reaction pH higher than about 6.5. For example, Figures 1b and 10e have about the same average particle size, but the difference in size distribution in these two samples can be noticed without any quantitative analysis. For a large size range, the size distribution of the resulting nanocrystals through two different strategies was compared using light scattering measurements (Figure 10f).

Figure 10f further indicates that the advantage of the new strategy in size distribution control became more apparent as the size of the nanocrystals increased. As pointed out in the previous paragraph, the nanocrystals in Figure 10f for the varying pH series were all grown with a relatively high pH, and it was thus through the nucleation-growth pathway. A better control on size distribution of the nanocrystals through the nucleation-growth pathway is actually not completely surprising, given that the size variation for the classic Frens method was achieved by three sequential steps: nucleation, aggregation, and intraparticle ripening (smoothing of the aggregates). Because aggregation played a role, the volume increase in this case should be stepwise, at least one particle a time, instead of atom-by-atom. Furthermore, the smoothing process (intraparticle ripening)[34] occurred at a nonuniform pace (Figure 3, bottom row). As a result, some of the nanocrystals were not spherical like the others. This nonuniformity in shape (see examples in Figures 1, 3, and 1S) would be averaged by light scattering measurements as an additional contribution to the size distribution values in Figure 10f. Again, to take advantage of this new approach, the reaction pH should be controlled roughly above 6.5. This choice of pH can largely avoid the nanowire aggregates as the intermediates as discussed earlier. The stability of the Au nanocrystals formed using this new approach was generally found to be similar to that of the Frens's method in terms of stability.

Discussion

Two distinguishable reaction pathways (Scheme 1) exist in synthesis of gold nanocrystals through citrate reduction using either the standard Frens strategy[20] or the varying pH strategy shown in Figure 10. The switching point of two growth

Scheme 1. Schematic Illustration of Two Reaction Pathways for Synthesis of Gold Nanocrystals by Citrate Reduction

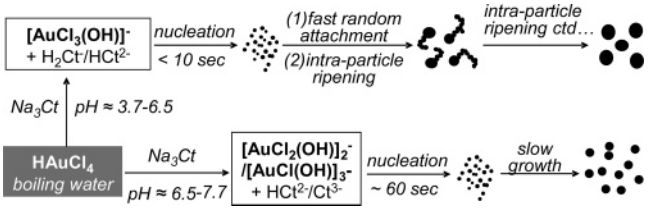

pathways is in the range from pH = 6.2 to pH = 6.5. The results in Figure 9 indicate that pH = 6.2 is the switching pH for the initial nucleation rates caused by the structural change of the gold complexes, from $AuCl_3(OH)^-$ to $AuCl_2(OH)_2^-$ (Figure 7, right). On the other hand, pH = 6.5 is the size switching point shown in Figure 1f (see replot of the data in the Supporting Information) and Figure 10. In Scheme 1, we temporarily adopt pH ≈ 6.5 as the switching point.

For the reaction route under high pH (Scheme 1, bottom), the data available in this report seem to be consistent with the traditional nanocrystal growth route, nucleation followed by a net growth stage that is diffusion-controlled. Such a route has been reasonably studied for synthesis of high-quality nanocrystals in nonaqueous solutions.[12] Although the nucleation-growth model was originally proposed by Turkevich et al.[19] and Frens[20] and more recently further developed by Kumar et al.,[25] there are two key differences between their model and the nucleation-growth route identified here. In Frens's report, he expected to increase the nucleation rate by increasing the concentration of Na_3Ct as a *reducing reagent*. This contradicts the results in Figures 2−5 and 9. The other difference is that the pH range encountered in the Frens method[19,20] actually falls into the other reaction pathway, which will be discussed later in the article.

When the pH in the reaction system was low (below about 6.5), which covers most of the $Na_3Ct/HAuCl_4$ ratios in the Frens method,[20] formation of final gold nanocrystals includes three consecutive but not well-separated steps. These three steps are nucleation, random attachment (or aggregation), and intra-particle ripening (or smoothing). The first two steps were quite fast (Figures 2, 3, 5c, and 9) in comparison to the reactions at higher pH values. The smoothing process through intra-particle ripening was very slow (Figure 4 and the related text). Intraparticle ripening[34] was first reported for CdSe nanocrystals occurring at about 300 °C. The driving force for such motion is to minimize the total surface energy of a nanocrystal.[34] The growth of the fat head with the shrinkage of the small tail nicely fits into this mechanism because the fat head has a relatively low chemical potential (or solubility).[34] For a soft metal such as gold, surface motion of the atoms would not be surprising at a relatively low reaction temperature, about 100 °C in the current system.

Evidence indicates that there was some rate difference between the two fast steps (i.e., nucleation and attachment). Along with the nanowires as intermediates, it was rare to see small dots (Figures 3, bottom panel, and 1S). This suggested that the random attachment process was faster than the nucleation process. When any new particles were formed, they would be attached to the existing nanowires immediately.

Attachment, or aggregation of the small nanocrystals, occurred largely in the low pH range (below about pH = 6.2−6.5). It is interesting to note that this pH is close to the main switching point of the initial reaction rate in Figure 9b,c. This means that the concentration of nuclei should be excessively high for these reactions with a low reaction pH, at least in comparison to the reactions at relatively high pH values. A large number of nuclei formed in a short period of time would create an environment for these small, and thus very reactive,[12] nuclei to encounter each other. This argument, purely based on particle concentration, is consistent with another experimental fact, that each reaction generated a stable and reproducible size (Figure 1f), instead of completely random and bulk-sized crystals. In other words, aggregation stopped when the concentration of the particles was lowered to a certain level. This implies a critical aggregation concentration of the gold particles, or a limit of particle density in a given solution, which is similar to the solubility concept of molecules in a solution.

The tendency of primary particles to form aggregates was studied by different research groups.[21−23,30,36,37] The AFM measurements by Zukoski et al. convincingly revealed that the citrate groups did adsorb onto gold surface and provide steric barriers for repulsion interactions. However, these repulsive interactions were lower when the pH was low.[26−28] In addition, the negative ζ-potential of gold nanocrystals in citrate solution showed a strong increase in magnitude upon the increase of the solution pH.[21,27] Although this needs to be further confirmed, this reduced surface charge could be a result of the pH-sensitive structures of the hydrolysis products of the citrate group (Figure 7). This means that the repulsive interaction between nanocrystals caused by the negative charges on each particle would be weak in the low pH range. As a result, aggregation may occur readily in the low pH range. Consistent with this hypothesis, the switching point (Figure 4S) was found to be around pH = 6.5 that is close to the pK_{a3} of citric acid. However, compared to the concentration argument discussed in the previous paragraph, this charge repulsion argument could not explain why the aggregation stopped at a given size for a given reaction.

Water as a solvent for synthesis of high-quality nanocrystals is unique. In the field of synthesis of high-quality nanocrystals in nonaqueous solution, there are two types of organic solvents. In the early days, coordinating solvents were dominating the field.[11] Later on, it was found that noncoordinating solvents have substantial advantages.[38] This is so because, when all solvent molecules are coordinating reagents (or ligands) to the nanocrystals and the related monomers, the reactivity of the monomers would be hardly tunable. It would thus be difficult to maintain a necessary balance between nucleation and growth, which is the key toward nanocrystals with a controlled size and shape.

Water is actually more complex than coordinating solvents discussed earlier. Water and its ionization products, H_3O^+ and OH^-, are common ligands for many metal ions. Furthermore, water can be a reactant as well. This point was reasonably proven even if synthesis of high-quality nanocrystals was performed in nonaqueous environment under 200−300 °C.[39,40] The last and also probably the most important aspect

(36) Privman, V.; Goia, D. V.; Park, J.; Matijevic, E. *J. Colloid Interface Sci.* **1999**, *213*, 36−45.
(37) Park, J.; Privman, V.; Matijevic, E. *J. Phys. Chem. B* **2001**, *105*, 11630−11635.
(38) Yu, W. W.; Peng, X. *Angew. Chem., Int. Ed.* **2002**, *41*, 2368−2371.
(39) Narayanaswamy, A.; Xu, H.; Pradhan, N.; Kim, M.; Peng, X. *J. Am. Chem. Soc.* **2006**, *128*, 10310−10319.

of water is that all chemicals in water can be readily integrated to a highly dependent chemical system. In the current case, Na_3-Ct was intentionally added as a reducing reagent and ligand. However, it changes the solution pH dramatically in the typical concentration range (Figure 7, left). This means a change of the existing form of water molecules, or the ratio between H_2O, H_3O^+, and OH^-. Consequently, the third component in the reaction system, auric acid, has been changed in structure as well. It results in new complexes of Au(III) in the reaction system with a certain amount of OH^- group as the ligands (Figure 7, right). The results in Figure 9 demonstrate that this structural change of Au(III) complexes substantially influences the reaction pathways (Scheme 1), the size and size distribution of the nanocrystals (Figure 10), and, to a certain degree, the shape of the nanocrystals (Figures 1, 3, and 10).

Conclusion

In summary, the solution pH in the current system seemed to influence the size, size/shape distribution, and the size/shape evolution pattern of the resulting gold nanocrystals. Three initial reactants (water, $HAuCl_4$, and sodium citrate) were thus integrated with each other. This implies that, more complex than a coordinating organic solvent, water might be considered as an integrating solvent. In the current system, the concentrations of $HAuCl_4$ and sodium citrate determined the solution pH, which in turn changed the structures of both reactants. When pH increased, the reactivity of Au(III) ions decreased substantially at pH = 6.2 and 7.2. Dependent on the reaction pH, gold nanocrystals could be formed through either the nucleation-growth pathway or nucleation-aggregation-smoothing pathway, with pH roughly being 6.2−6.5 as the switching point. All results in this report revealed that, in addition to being the reducing reagents and protection ligands, sodium citrate has played the third equally important role in the current synthetic system: as pH mediator. With this understanding, it was possible to synthesize nearly monodisperse gold nanocrystals with sizes from 20 to 40 nm by simply varying the solution pH.

Experimental Section

Materials. All water was distilled and subsequently purified to Millipore Milli-Q quality. All glassware used was cleaned in a bath of freshly prepared aqua regia solution (HCl/HNO_3, 3:1), then rinsed thoroughly with H_2O before use. Auric acid ($HAuCl_4$), trisodium citrate ($Na_3C_6H_5O_7$), sodium chloride (NaCl), sodium hydroxide (NaOH), and hydrochloric acid (HCl) were of analytical grade and were not purified further before use.

Synthesis of Gold Nanoparticles. A typical reaction is as follows. A 100-mL sample of aqueous $HAuCl_4$ (0.25 mM) was prepared in a 250-mL flask, containing controlled amounts of HCl or NaOH at room temperature. The solution was brought to boil while being stirred, and the corresponding amount of 5% aqueous sodium citrate with initial molar ratio of citrate to Au^{3+} was added. The reaction was allowed to run until the solution reached a wine red color, indicating the reaction was completed. The initial $HAuCl_4$ concentration was varied from 0.125 to 1 mM. For the reactions in the series of variable $Na_3Ct/HAuCl_4$ ratios were performed by varying the concentration of Na_3Ct with a fixed $HAuCl_4$ concentration. The reactions in the series of variable pH were carried out by adding either HCl (1 M) or NaOH (1 M) into the reaction solution before the addition of Na_3Ct.

UV−Vis Absorption Spectroscopy. UV−vis absorption spectroscopy of gold nanocrystals was recorded on a Varian Cary 100 spectrophotometer. At different time intervals, aliquots of the solution were taken out and the samples were cooled in ice water to quench the reaction.

Transmission Electron Microscopy. TEM and HRTEM images were taken on a Hitachi H-8100 IV at 200 kV and JEOL-JEM-3010 at 300 kV electron microscope. Point-to-point resolution of the HRTEM was 0.14 nm. Samples for Hitachi H-8100 IV were prepared by dipping a drop of the colloidal solution (the aliquots taken during the course of a reaction) onto a Formvar-coated copper grid. Specimens for HRTEM were prepared by depositing a drop of colloidal solution onto holey carbon-coated Cu grids.

Dynamic Light Scattering. DLS analyses were performed on a Brookhaven BI-90Plus particle size analyzer with a scattering angle of 90°.

Acknowledgment. All experimental work was performed at Jilin University, and related financial support was partially provided by the National Natural Science Foundation of China, the Program for NCET in University of Chinese Ministry of Education, and the National Science Foundation. We are grateful for the help of Mr. Daliang Zhang on HRTEM.

Supporting Information Available: Supporting results mentioned in the text, including Figures 1S−4S. This material is available free of charge via the Internet at http://pubs.acs.org.

JA074447K

(40) Ould-Ely, T.; Prieto-Centurion, D.; Kumar, A.; Guo, W.; Knowles, W. V.; Asokan, S.; Wong, M. S.; Rusakova, I.; Luettge, A.; Whitmire, K. H. *Chem. Mater.* **2006**, *18*, 1821−1829.